Polypyrrole-Pt nanocomposites as electrochemical glucose sensor

Nitin R. Dighore, Suresh T. Gaikwad, Anjali S. Rajbhoj*

Department of Chemistry, Dr. Babasaheb Ambedkar Marathwada University, Aurangabad 431004, India

*Corresponding author. Tel: (+91) 240-2403311; Fax: (+91) 240-2403335; E-mail: anjali.rajbhoj@gmail.com

ABSTRACT

A voltammetric sensor was developed for detection of glucose by using cyclic voltammetry (CV). The sensing platform was Polypyrrole-Pt nanocomposites on Platinum electrode (PPy-Pt-PtE). PPy-Pt was synthesized by chemical method, using $FeCl_3$ oxidant. XRD, SEM and TEM results showed that PPy doped with Pt were highly porous, nanocrystalline composites. The PPy-Pt-PtE modified electrode observed reversible behavior with ferricyanide system which had about 2.05 times more surface area and exhibited higher currents for glucose oxidation compared to bare PtE. Glucose was sensed in the range of 100mM to 1000 mM from the linear regression plotted $R^2= 0.990$ and $R^2=0.994$ the sensitivity was found to be 0.047 mA/mM~cm^2 and 0.0445 mA/mM~cm^2. These results indicate that PPy-Pt-PtE exhibited good platform and could be used for voltammetric determination of glucose. Copyright © 2016 VBRI Press.

Keywords: PPy-Pt nanocomposite; electrochemical analysis; glucose sensor; cyclic voltammetry.

Introduction

Diabetes is a widespread but treatable metabolic disease has affected millions of people all over the world [1]. Early detection and treatment of diabetes require tight monitoring of blood glucose level to prevent long term complication such as heart attack, kidney disease and blindness. Therefore, there is increasing demand for glucose sensors with high sensitivity, excellent selectivity, good stability, fast response and a low cost since last decade. The conventional enzymatic glucose sensor exhibits high sensitivity and selectivity [2-4], but enzymatic detection most serious problem and there is lack of stability as it is affected by pH, temperature & humidity [5]. Furthermore, enzymatic sensors suffer from high cost and require complicated procedure. Much work has been carried out to develop enzyme free glucose sensors [6-8]. Enzymeless sensing is an important area of sensor development which plays an important role to develop; robust, lifelong systems used in this direction by using metal nanocomposites.

Conducting polymer and metal nanoparticles have potential to combine two borderline technologies to yield with conducting polymer nanocomposites materials with improved properties. Conducting polymer has characteristic properties to combine with the various materials because of the redox behavior. Conducting polymers have prospective as good conductors [9], long range application in sensor [10-11], solar cell [12], electrochromic devices [13], light emitting diode [14] and energy storage devices [15]. Nobel metal such as Au, Pt, Pd and metal oxide nanoparticles have widely used as sensing materials for non-enzymatic glucose sensors. Most of these electrodes have drawbacks of low sensitivity, poor selectivity and stability because of surface poisoning from absorbed intermediate and poor electrical conductivity.

One of the major strategies to enhance charge transfer in electrochemical biosensor is to design composite materials by combining highly electrocatalytic materials with conducting substance. Now a day, conducting polymer incorporated with metal nanoparticles have attracted much more attention for the development of electrocatalytic system [16]. Recently there has been wide interest in the field of conducting polymer modified electrode as it exhibited more porous structure [17-18]. Among the conducting polymers, polypyrrole (PPy) has good mechanical and chemical stability, easy preparation and most promising member for application in electrocatalytic as well as other purposes [19-20]. PPy has been successfully applied as conducting matrixes of composite material incorporating with SeO_2 [21], CeO_2 [22], GaN [23], Co [24] and noble metals such as Au [25], Ag [26-27], Pd [28] and Pt [29].

In the present study it was observed that chemically synthesized conducting polymer PPy-Pt nanocomposites have received less attention and we have decided to use synthesized PPy-Pt nanocomposites as modified electrode in cyclic voltammetry method for electrochemical detection of glucose.

Experimental

Materials

Pyrrole (Spectrochem), ferric chloride (SD-Fine Chem.), Hexa chloro platinic acid (Sigma-Aldrich) and sodium citric acid (SD-Fine chem.) were purchased and use as such as without further purification. All solutions were prepared in double distilled water.

Synthesis of Pt Nps, PPy and PPy-Pt nanocomposites

In round bottom flask, 100 ml tri sodium citrate (0.1M) solution was heated upto 80 °C. Hexa chloro platinic acid H_2PtCl_6 (0.01M) solution was added drop wise into the preheated tri sodium citrate solution. The mixture was refluxed with continuous stirring for 4 Hrs. The resulting

solution showed a change in color from yellow orange to bright brown indicating formation of Pt nanoparticles. The solution was allowed to cool and settle for 12 hrs. Pt nanoparticles were separated by simple decantation. The obtained Pt nanoparticles were washed 2-3 times with distilled water then with acetone and dried in vacuum desiccator. The dried Pt nanoparticles were stored at ambient temperature in air tight glass container.

Synthesis of pure polypyrrole (PPy) was done by chemical method. The reaction was carried out at 5 ºC [30]. The ratio of monomer (pyrrole): oxidant (FeCl₃) was 1:2.4 [31]. The mixture was stirred for 4 hours and was then kept unagitated for 24 hours so that PPy powder settled down. The PPy powder was filtered out under vacuum and washed with distilled water several times to remove impurities if any. The PPy was dried for 2 days at room temperature. The doping of Pt nanoparticles in PPy was done by addition of 500 mg Pt nanoparticles in pyrrole solution and stirred for 30 min and then oxidant FeCl₃ was added to polymerization reaction. The mixture was stirred for 4 hours and then it was kept unagitated for 24 hours so that Pt-Ppy nanocomposites powder settled down. The Ppy-Pt-nanocomposites powder was filtered out under vacuum and washed with distilled water and acetone 3 - 4 times to remove any impurities. The Ppy-Pt-nanocomposites were dried for 2 days at room temperature. The dried PPy-Pt-nanocomposites were stored at ambient temperature in air tight glass container.

Preparation of modified electrode

The platinum (Pt) electrode (2 mm diameter) was carefully polished using a polishing cloth with alumina slurry and then rinsed thoroughly with glass distilled water. The Pt electrode was then placed in ultrasound cleaner for 5 min, rinsed again with glass distilled water and allowed to dry at room temperature. To prepare the Pt electrode modified with PPy-Pt nanocomposites, an alcoholic solution of 0.1 % Nafion dispersion of PPy-Pt nanocomposite (1 mg mL⁻¹) was prepared and the suspension (5mL) was cast on to the surface of pretreated Pt electrode. The solvent was allowed to evaporate at room temperature which resulted into immobilized PPy-Pt nanocomposite material on the Pt electrode surface.

Characterizations

The prepared nanocomposite materials of PPy and Pt nanoparticles were characterized by XRD, SEM & TEM techniques. The X-ray powder diffraction patterns of Pt Nps and Ppy-Pt nanocomposites were recorded on Bruker 8D advance X-ray diffractometer using CuKα radiation of wavelength = 1.54056 Å. To study the- morphology and elemental composition of Pt nanoparticles, PPy and PPy-Pt nanocomposites were examined using SEM. The SEM analysis was carried out with JEOL; JSM- 6330 LA operated at 20.0kV and 1.0000 nA. Shape, size, morphology was calculated by TEM analysis carried out on Philips model CM200 operated at 200kV.

Cyclic voltammetry (CV) measurements were performed on a Metrohm Autolab PGSTAT128N (Metrohm B.V., Utrecht, Netherlands). One compartment with three electrode system consists of a saturated Ag/AgCl reference electrode, a platinum wire auxiliary electrode and a modified Pt electrode as working electrode. Glucose measurement was carried out in 0.1 M NaOH at RT. For the CV measurements, the potential scan was taken from -0.80 to 1.00 V at scan rate 100 mVs⁻¹. The CV measurements were carried out at different concentration of glucose in the range of 100 to 1000 mM and also the different scan rate was studied in the range 25 to 150 mVs⁻¹.
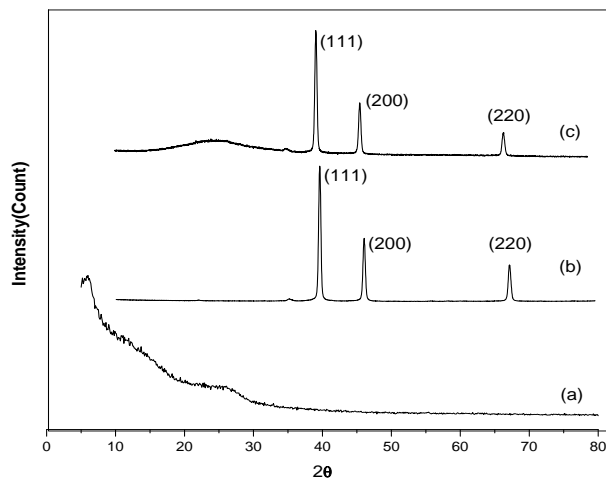
Fig. 1. XRD patterns of a) PPy, b) Pt nanoparticles and c) PPy-Pt-nanocomposites.

Results and discussion

X-ray diffraction (XRD)

X-ray diffraction studies show that PPy powder is amorphous in nature as shown in **Fig. 1(a)**. The broad peak was observed at about 2θ=27° which is characteristic of amorphous PPy which shows the scattering due to Ppy chains at inner planar spacing [32]. The average chain separation can be calculated from these maxima using the relation [33-35]. The average chain separation (R) was found to be 4.12 A° for pure PPy. From **Fig. 1(b)** XRD pattern of pure Pt Nps strongly oriented cubic crystal structure a=b=c=3.923 & α=β=γ= 90, (JCPDS card No. 04-0802), strong and intense peaks at (111), (200) and (220) show crystalline nature of Pt nanoparticles. The X-ray diffraction pattern after doping of Pt nanoparticles is shown in **Fig. 1(c)**. The coating of Ppy on Pt nanoparticles leads to the formation to sharp peak and decrease in peak intensity than pure Pt nanoparticles which confirm the formation of PPy-Pt crystalline nanocomposites.

The average particle size was calculated by using Debye-Scherrer [36-37] formula, indicating nanoparticles are having high surface area. XRD pattern of pure Pt Nps and PPy-Pt nanocomposite show intense peaks at (111), (200) and (220) plane and full width of half maximum (FWHM) values in **Table S1**. The average crystalline size of Pt Nps and PPy-Pt were found to be 22.096 nm & 20.044 nm respectively.

Scanning electron microscope

The surface morphological images shown in **Fig. 2(a-c)** are of PPy, Pt Nps and Ppy-Pt nanocomposites respectively. **Fig. 2(a)** shows globular structures of PPy, the individual

granules observed were nearly spherical and have a close packing. It seems that such spherical particles were one over the other forming a continuous structure. The image of **Fig. 2(b)** shows the microporous structure of Pt Nps. In **Fig. 2(c)** clearly exhibits the doping of Pt Nps on PPy to form PPy-Pt nanocomposites. It also shows the effective incorporation of Pt Nps on highly microporous nature of PPy-Pt nanocomposites. The quantitative and qualitative analysis was done by EDS spectrum as shown in **Fig. 2(f)**. The elemental distribution of Pt NPs was Pt 86.08 wt%, C 3.55 wt% and O 8.40 wt% respectively. The EDS spectrum results of elemental composition of PPy-Pt nanocomposites is shown in **Fig. 2(g)** which showed Pt 78.75 wt%, C 11.25wt%, N 3.41 wt% and O 3.15wt%. From the EDS data the formation of Pt NPs and PPy-Pt nanocomposites was confirmed.
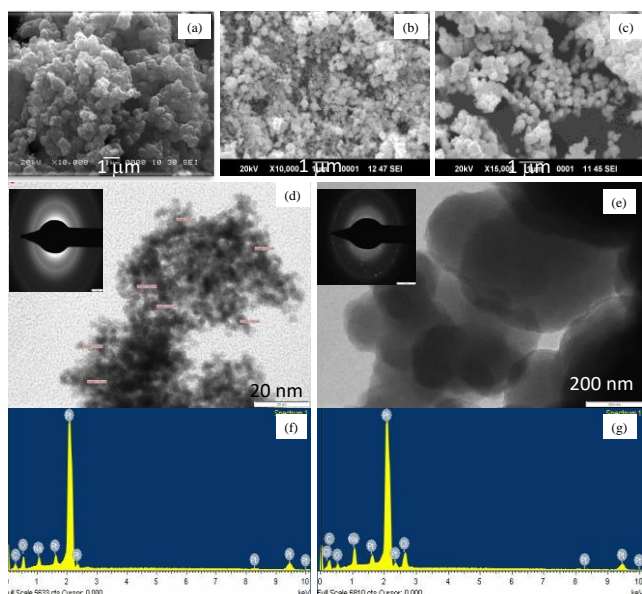
Fig. 2. SEM images of a) PPy, b) Pt Nps and c) PPy-Pt-nanocomposites, TEM images of d) Pt- Nps e) PPy-Pt nanocomposites with inset of SAED pattern, EDS spectra of f) Pt Nps and PPy-Pt nanocomposites.

Transmission electron microscope

The TEM images depicted in **Fig. 2(d, e)** is a direct morphological observation of Pt NPs and PPy-Pt nanocomposites. The average overall dimensions of Pt Nps and PPy-Pt nanocomposites were found to be 10 nm and 50 nm respectively. The shapes of Pt Nps were spherical while PPy-Pt nacomposites (**Fig. 2e**) showed Pt Nps deposited on porous Ppy. In the inset **Fig. 2(d, e)** SAED pattern indicate Pt Nps and PPy-Pt nanocomposites were crystalline in nature. The inter planner spacing in Pt Nps obtained from SAED pattern was 0.2254 nm which agreed with the (111) lattice spacing of FCC Pt (0.2264 nm from XRD). The inter planner spacing (hkl) in PPy-Pt nanocomposites obtained from SAED pattern were 0.2551 nm (111), 0.2181 nm (200) and 0.1638 nm (211) which are in good agreement with lattice spacing obtained from XRD.

Electrochemical analysis

The electrochemical behavior of bare PtE and PPy-Pt-PtE were studied by cyclic voltammetry in 0.1 mM ferricyanide at the scan rate 100 mV/s. The cyclic voltammograms depict that the Pt-PPy-PtE showed higher currents in 0.1 mM ferricyanide compare to the bare PtE.
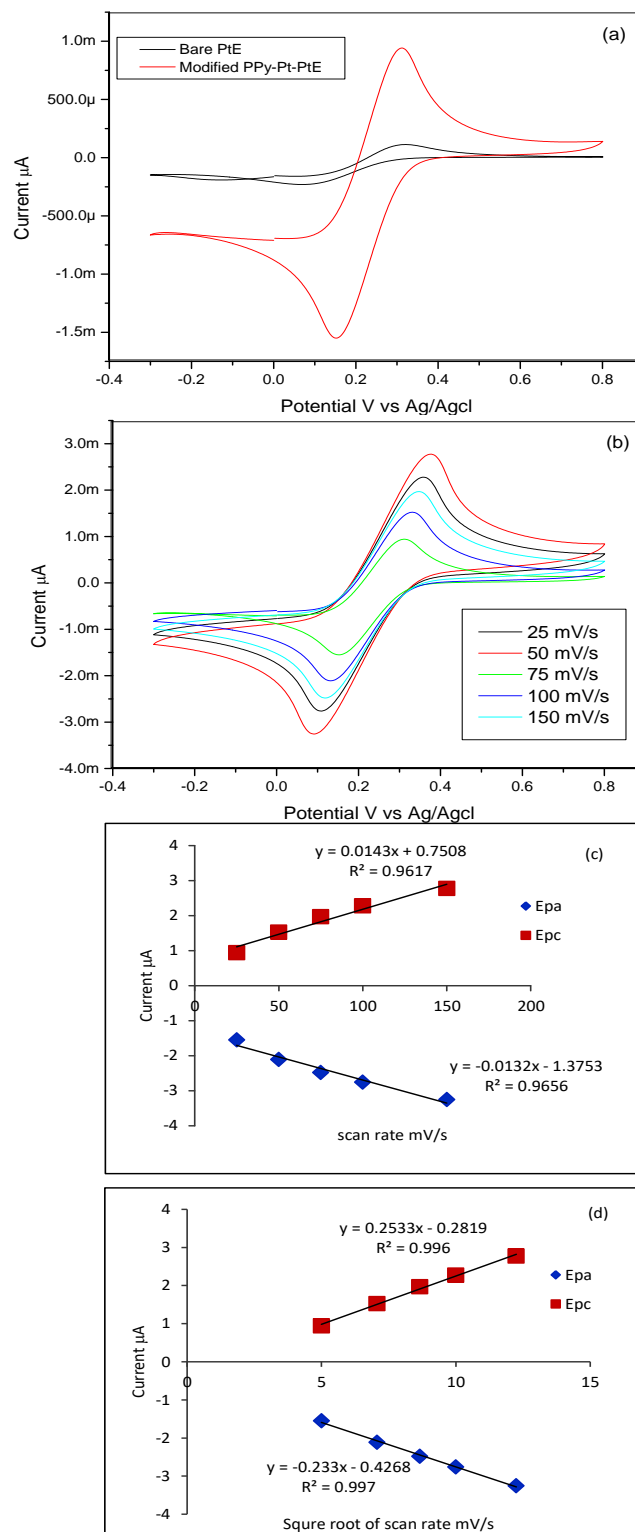
Fig. 3. (a) Cyclic voltammetry of bare PtE (black) andPPy-Pt-PtE (red) in 0.1mM $K_3Fe(CN)_6$ in 0.1 KNO_3 solution of scan rate 100 mV/s. (b) Cyclic voltammetry response of PPy-Pt-PtE at different scan rate in 0.1 mM K_3FeCN_6 in 0.1 KNO_3 solution at scan rate from 25,50,75,100, 150 mV/s. Influence of the potential scan rate on the electrochemical response of 0.1 mM K_3FeCN_6 in 0.1 KNO_3at PPy-Pt-PtE. The plot of peak current versus scan rate (c) and the square root of scan rate (d).

The increase peak currents are largely the result of increased electroactive surface area of the Pt-PPy-PtE.

Using diffusion coefficient 6.8×10^{-6}cm^2/s [38], and Randeles Sevick equation, it was seen that the electroactive surface area for modified PPy-Pt-PtE was found to be 2.05 times higher than that of bare electrode **Fig. 3(a)**. The effect of scan rate on the oxidation and reduction current on PPy-Pt-PtE was investigated by cyclic voltammetry in 0.1 mM ferricyanide at different scan rate in 25-150 mV/s in the potential range -0.2V to 0.9V **Fig. 3(b)**. The anodic and cathodic peak potential varied linearly with logarithm of scan rate (**Fig. 3c**) while the oxidation and reduction peak currents linearly increase with the square root of scan rate **Fig. 3(d)**. This further confirmed that PPy-Pt-PtE shows reversible behavior in known reversible redox systems such as ferricyanide system.
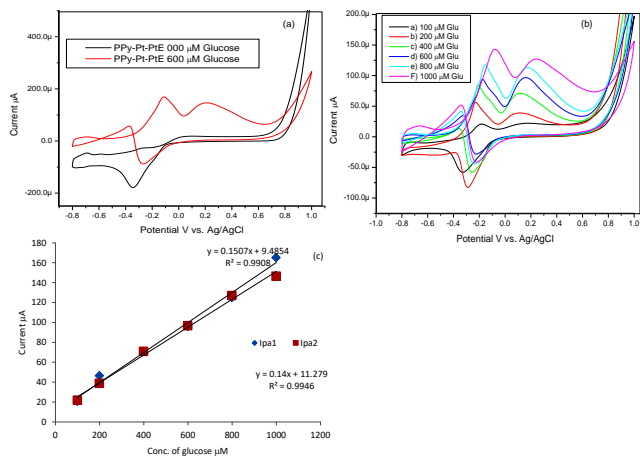
Fig. 4. (a) Cyclic voltammetry of without (black) and with (red) 600 mM of glucose in 0.1 NaOH solution of scan rate 100 mV/s at Pt-PPy-PtE. (b) Cyclic voltammetry response of Pt-PPy-PtE electrode in 0.1 NaOH solution containing a) 000 mM b) 200 mM c) 400 mM d) 600 mM e) 800 mM and f) 1000 mM of glucose at scan rate from100mV/s vs. Ag/AgCl. (c) Influence of the potential scan rate on the electrochemical response of 0.1 M NaOH in 600 mM glucose at PPy-Pt-PtE. The plot of peak current versus square root of scan rate Ipai and Ipaii.

In order to investigate the electrocatalytic oxidation activity of PPy-Pt modified PtE in 0.1 M NaOH solution, the CV results of the PPy-Pt-PtE are studied in presence and absence of 600 µM glucose in 0.1 NaOH at scan rate 100mV/s in potential range -0.8V to 1.0V. The CV recorded in the 0.1 M NaOH with 600 µM glucose is presented in **Fig. 4(a)**. The characteristic changed significantly, during the positive scan three peaks appeared using the PPy-Pt modified PtE. The first peak at -0.69 V was due to the electrochemical adsorption of glucose, the second peak appearing at -0.14 V was result of electrosorption of glucose to form gluconic acid by releasing one proton [39]. The third peak appearance at 0.20 V was due to accumulation of intermediate on the electrode surface forming a product such as glucano lactone or gluconic acid. The decrease in the current at more positive potential was caused by the formation of Pt oxide and during the negative scan with the reduction of Pt oxide at potential around -0.25V was due to the surface side which would be reactivated and available for the direct oxidation of glucose resulting in a sharp increase in anodic current with peak at -0.34 V. The applied potential moved to more negative values because of the electrosorption of

glucose at again the PPy-Pt, resulting in an accumulation of intermediates on the electrode surface which led to the decreasing in anodic current.

A cyclic voltammetry electrochemical sensor was developed for detection of glucose. **Fig. 4(b)** shows the obtained cyclic voltammograms at PPy-Pt electrode for different concentration from 100mM to 1000 mM in 0.1 M NaOH. The first and second oxidation peak current was directly proportional to the concentration of glucose. The calibration for first and second peak current against the concentration of glucose was plotted in **Fig. 4(c)** with linear regression equation of with R^2= 0.990 and R^2= 0.994 and the sensitivity was found to be 0.047 mA/mM.cm^{-2} and 0.0445 mA/mM.cm^{-2}.
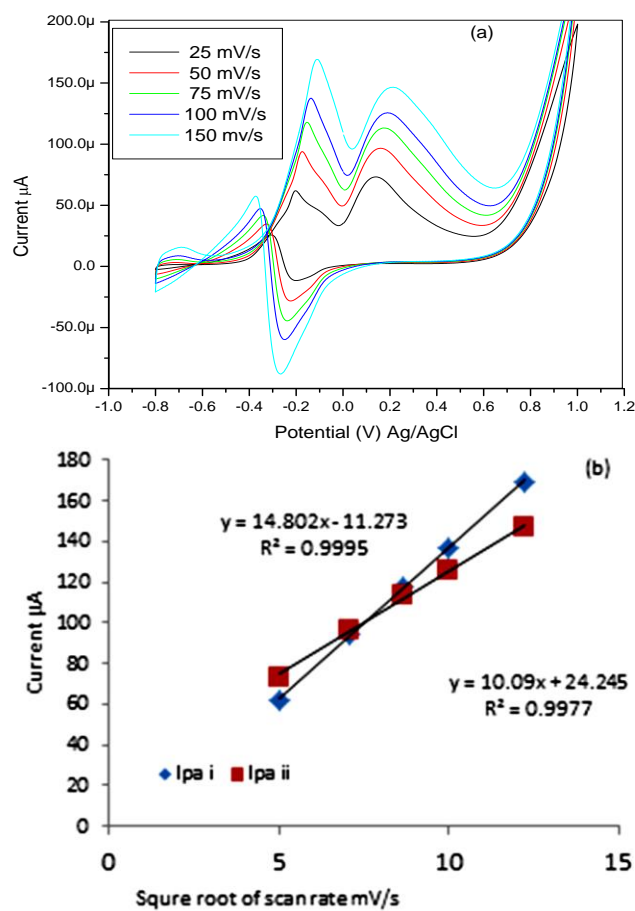
Fig. 5. (a) Cyclic voltammetry response of Pt-PPy-PtE at different scan rate in 0.1 NaOH solution in 600 µM of glucose; scan rate from 25, 50, 75, 100, 150 mV/s (b) Influence of the potential scan rate on the electrochemical response of 0.1 M NaOH in 600 µM glucose at PPy-Pt-PtE. The plot of peak current versus square root of scan rate Ipai and Ipaii.

The effect of scan rate on the oxidation current on PPy-Pt-PtE was investigated by cyclic voltammetry in 600 mM glucose in 0.1 M NaOH at different scan rate in 25-150 mV/s in the potential range -0.8 to 1 V (**Fig. 5a, b**). The reproducibility of PPy-Pt was also investigated by performing cyclic voltammetric analysis in solution containing 600mM glucose in 0.1 M NaOH for five different scan rates the standard deviation was 4.09 % which indicate that electrode reproducibly determines the presence of glucose.

Conclusion

We have successfully synthesized the Pt Nps and Ppy-Pt nanocomposites which are simple, nontoxic, porous and in green solvent water. The SEM image shows porous structure of PPy-Pt nanocomposites and EDS spectrum depicts the percentage the formation of PPy contains Pt nanocomposites. The Pt NPs and PPy-Pt nanocomposites were crystalline in nature and the average crystallite size was found to be 22.096 nm and 22.044 nm respectively. From TEM images the Pt Nps and PPy-Pt nanocomposites average size obtained was 10nm and 50nm. In Ppy-Pt NPs, inter planner spacing from SEAD pattern was in good agreement with XRD pattern. The electrochemical analysis of PPy-Pt- PtE modified electrode showed good activity as a glucose sensor. The results obtained from cyclic voltammetry methods shows that PPy-Pt-PtE modified electrode was used to direct oxidation of glucose. The good electrocatalytic ability, good sensitivity and easy fabrication make PPy-Pt-PtE as excellent electrochemical sensor for glucose detection.

References

1. Sljukic, B.; Banks, C.; Salter, C. Crossley, A.; Richard, G; *Compton Analyst.,* **2006**, *131*, 670.
   DOI: 10.1039/B601299J
2. Gao, G.; Chen, Q.; Chen, X. *Sci. China. Chem.*, **2011**, *54*, 1777.
   DOI:10.1007/s11426-011-4389-5
3. Tiwari, A., Terada, D., Yoshikawa, C., Kobayashi, H., *Talanta*, **2010**, 82 (*5*), 1725-1732.
   DOI: 10.1016/j.talanta.2010.07.078
4. Wilson, R.; Turner, A.; *Biosens. Bioelectron.* **2009**, *7*, 165.
   DOI:10.1016/0956-5663(92)87013-F
5. Abun, S.; Bang, G. S.; Koga, T.; Nonka, Y.; Sotomura, T.; Taniguch, I. *Electrochem. Commun.,* **2003**, *5,* 317.
   DOI: 10.1016/S1388-2481(03)00055-9
6. Wang, J. *Electroanal.***2001**, *13*, 983.
   DOI: 10.1002/1521-4109(200105)13:8/9<635
7. Safavi, A.; Maleki, S. M.; Farjami, E. *Biosen. Bioelectron*., **2009**, *24*, 1655.
   DOI: 10.1016/j.bios.2008.08.040.
8. Wu, G.H.; Song, X.H.; Wu, Y. F.; Chen, X. M.; Luo, F.; Chen, X. *Talanta*, **2013**, *105*, 379.
   DOI: 10.1016/j.talanta.2012.10.066
9. Gangopadhyay, R.; De, A. *Chem. Mater.* **2000**, *12*, 608.
   DOI: 10.1021/cm990537fCCC.
10. Zhang, T.; He, Y.; Wang, R.; Geng, W. *Sens. Actuators B,* **2008**, *131*, 687.
    DOI:10.1016/j.snb.2007.12.059.
11. Majid, K.; Tabassum, R.; Shah, A.F.; Ahmad, S.; Singla, M. L. *J. Mater. Sci. Mater. Electron*. **2009**, *20*, 958.
    DOI: 10.1007/s10854-008-9817-8
12. Tan, S.; Zhai, J.; Xue, B.; Wan, M., Meng, Q.; Li, Y. *Langmuir,* **2004**, *20*, 2934.
    DOI:.10.1021/la036260m CCC.
13. Hu, H.; Hechavarrıa L.; Campos J. *Solid State Ionics* **2003**,*161*,165.
    DOI: 10.1016/S0167-2738(03)00214-5
14. Huang, J.; Wang, X.; De Mello, A.J.; De Mello, J.C.; Bradley, D.D.C. *J. Mater. Chem.* **2007**, *17*, 3551.
    DOI:10.1039/B705918N.
15. Gurunathan, A.V. Murugan, R. Marimuthu, U.P. Mulik, D.P. Amalnerkar, *Mater. Chem. Phys.* **1999**, *61*, 173. PII: S 0254-0584(99)00081-4
16. Jiwei, L.; Jingasia, Q.; Miao, Y.; Chen, J. *J. Mater. Sci*., **2008**, *43*, 6285.
    DOI: 10.1007/s10853-008-2905-6
17. Wallace, G. C.; Smyth, M.; Zhao, H. *TrAC Trends in Analytical Chem.*, **1999**, *18*, 245.
    DOI: 10.1016/S0165-9936(98)00113-7
18. Kamada, K.; Kamo, J.; Motonaga, A.; Iwasaki, T.; Hosokawa, H. *Polymer Journal*, **1994**, *26*, 833.
    DOI:10.1295/polymj.26.833
19. Valsesia, A; Lisboa, P; Colpo, P; Rossi, F; *Anal. Chem*., **2006**, *78*, 7588.
    DOI: 10.1021/ac0609172
20. Ramanavicius, A.; Ramanaviciene, A.; Malinausks, A. *Electrochemica Acta.,* **2006**, *51*, 6025.
    DOI: 10.1016/j.electacta.2005.11.052
21. Khanna, P.K.; Bhanoth, S.; Dhanwe, V.; Kshirsagar, A.; More, P. *RSC Adv*., **2015**, *5*, 92818.
    DOI: 10.1039/C5RA14425F
22. Wang, X.; Wang, T.; Liu, D.; Guo, J.; Liu, P. Ind. *Eng Chem Res*., **2016**, *55*, 866.
    DOI: 10.1021/acs.iecr.5b03891
23. Munusamy, S.; Suresh, R.; Giribabu, K.; Manigandan, R.; Praveen Kumar, S.; Muthamizh, S.; Bagavath, C.; Stephen, A.; Kumar, J.; Narayan, V.; *Arabian Journal of Chem.,* **2015**, (In Press)
    DOI: 10.1016/j.arabjc.2015.10.012
24. Bocchetta, P.; Gianoncelli, A.; Abyaneh, M. K.; Kiskinova, M.; Amati, M.; Gregoratti, L.; Jezersek, D.; Mele, C.; Bozzini, B. *Electrochemica Acta*., **2014**, *137*, 535.
    DOI: 10.1016/j.electacta.2014.05.098
25. Ashassi-Sorkhabi, H.; Bagheri, R.; Rezaei-Moghadam, B. *Journal of Appl. Polymer Sci.,* **2014**, *131*, 41087.
    DOI: 10.1002/app.41087
26. Praveenkumar, K.; Sankarappa, T.; Ashwajeet, J. S.; Ramanna, R. *Journal of Polym*, **2015**, 893148.
    DOI: 10.1155/2015/893148
27. Kumar, V.; Ali, Y.; Sharma, K.; Kumar, V.; Sonkawade, R.G.; Dhaliwal, A.S.; Swart H.C. *Nucl. Inst. Methods in Phys. Res. B*, **2014**, *233*,7.
    DOI: 10.1016/j.nimb.2014.01.009.
28. Fujii, S.; Hamasaki, H.; Abe, H.; Yamanaka, S.; Ohtaka, A.; Nakamura, E.; Nakamura, Y. *J. Mater. Chem. A*, **2013**, *1*, 4427.
    DOI: 10.1039/C3TC30853G
29. Lemos, H. G.; Santos, S. F.; Venancio, E. C. *Synthesis Metals*, **2015**, *203*, 22.
    DOI: 10.1016/j.synthmet.2015.02.006
30. Jiang, L.; Jun, H. K.; Hoh, Y. S.; Lim, J. O.; Lee D. D.; Huh, J. H. *Sensors and Actuators B: Chemical*, **2005**, *105*, 132.
    DOI: 10.1016/j.snb.2004.05.015
31. Armes, S. P. *Synthetic Metals,* **1987**, *20*, 365.
    DOI: 10.1016/0379-6779(87)90833-2
32. Ouyang, J.; Li, Y. *Polymer,* 1997, 38, 1971.
    DOI:10.1016/S0032-3861(96)00749-5
33. Alexander, L. E.(Eds); X-ray diffraction methods in polymer science, John Wiley, New York, **1969**.
34. Cheah, K.; Forsynth, M.; Troung, V. T. *Synth. Met*., **1999**, *101*, 19.
    DOI: 10.1016/S0379-6779(98)00790-5
35. Lamon, P.; Haigh, J.; *Mat. Res. Bull*., **1999**, *34*, 665.
    DOI: 10.1016/S0025-5408(99)00069-0
36. Cheah, K.; Forsyth, M.; Troung, V.T. *Synth. Met*., **1998**, *94*, 215.
    DOI: 10.1016/S0379-6779(98)00006-X
37. Reetz, M. T.; Helbig, W. J. *Am.Chem. Soc*., **1994**, *116*, 740.
    DOI: 10.1021/ja00095a051
38. Borgohain, K.; Murase, N.; Mahamuni, S. *J. Apply. Phy.* **2002**, *92*, 1294.
    DOI: 10.1063/1.1491020
39. Yuan, Y.; Wallace, G.G.; John, R.; Adeloju S.B. *Polymer Gels Networks,* **1998**, *6*, 383.
    DOI:10.1016/S0966-7822(98)00034-3
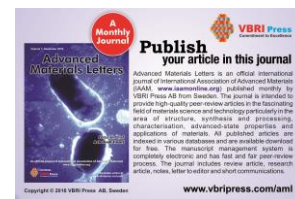
Supporting information

Table S1. Average crystalline size of Pt Nps & PPy-Pt nanocomposites.

S. no.	Nanoparticles	2θ/degree	h k l	FWHM	Size (nm)	Average Size (nm)
1	Pt-NPs	39.776	111	0.3869	23.605	22.096
		46.260	200	0.3997	22.798	
		67.496	220	0.4548	19.885	
2	PPy-Pt Nps	39.745	111	0.3967	22.982	20.044
		46.245	200	0.4392	20.63	
		67.557	220	0.5433	16.52	